Molecular Therapy
Original Article

Characterization of circRNA-Associated-ceRNA Networks in a Senescence-Accelerated Mouse Prone 8 Brain

Shuai Zhang,[1,2,3] Dina Zhu,[1,2,3] Hong Li,[1,2,3] Hejian Li,[1,2,3] Chengqiang Feng,[1,2,3] and Wensheng Zhang[1,2,3,4]

[1]Beijing Area Major Laboratory of Protection and Utilization of Traditional Chinese Medicine, Beijing Normal University, Beijing 100088, China; [2]Engineering Research Center of Natural Medicine, Ministry of Education, Beijing Normal University, Beijing 100088, China; [3]Faculty of Geographical Science, College of Resources Science & Technology, Beijing Normal University, Beijing 100088, China; [4]National & Local United Engineering Research Center for Sanqi Resources Protection and Utilization Technology, Kunming 650000, China

Alzheimer's disease (AD) is one of the most common neurodegenerative diseases. Although many researchers have attempted to explain the origins of AD, developing an effective strategy in AD clinical therapy is difficult. Recent studies have revealed a potential link between AD and circRNA-associated-ceRNA networks. However, few genome-wide studies have identified the potential circRNA-associated-ceRNA pairs involved in AD. In this study, we systematically explored the circRNA-associated-ceRNA mechanism in a 7-month-old senescence-accelerated mouse prone 8 (SAMP8) model brain through deep RNA sequencing. We obtained 235 significantly dysregulated circRNA transcripts, 30 significantly dysregulated miRNAs, and 1,202 significantly dysregulated mRNAs. We then constructed the most comprehensive circRNA-associated-ceRNA networks in SAMP8 brain. GO analysis revealed that these networks were involved in regulating the development of AD from various angles, for instance, axon terminus (GO: 0043679) and synapse (GO: 0045202). Following rigorous selection, we discovered that the circRNA-associated-ceRNA networks in this AD mouse model were mainly involved in the regulation of Aβ clearance (Hmgb2) and myelin function (Dio2). This research is the first to provide a systematic dissection of circRNA-associated-ceRNA profiling in SAMP8 mouse brain. The selected circRNA-associated-ceRNA networks can profoundly affect the diagnosis and therapy of AD in the future.

INTRODUCTION

Circular RNA (circRNA) has become a research focus in the field of non-coding RNA. By contrast to linear RNA, circRNA forms a covalently closed-loop structure without 5′-3′ polarity and poly(A) tail.[1,2] circRNA is more resistant to exonuclease than linear transcript and is therefore more stable in cells.[3,4] circRNA inhibits the function of microRNA (miRNA) as miRNA sponges through the competing endogenous RNA (ceRNA) network.[5] The circRNA-associated-ceRNA network may play a key role in many disease processes. Huang et al.[6] reported that circRNA MYLK competitively binds with miRNA-29a-3p and thus increases expression of the target genes DNMT3B, VEGFA, and ITGB1, which are involved in the progression of bladder cancer. Fan et al.[7] summarized the function and role of circRNA as a biomarker in cardiovascular diseases. circRNA-ZNF609 functions as a ceRNA to regulate AKT3 expression by sponging miR-150-5p in Hirschsprung's disease.[8] As a new form of post-transcriptional control, this network has a great potential implication in disease research. In addition, growing evidence suggests that circRNAs are highly enriched in mammalian brain tissues and are often derived from the genes specific for neuronal function.[9] Given these findings, exploring the role of the circRNA-associated-ceRNA network in neurodegenerative disorders such as Alzheimer's disease (AD) is necessary.

AD is the most common form of dementia, characterized by age-dependent memory loss and impairments of multiple cognitive functions.[10–12] Although many research efforts have tried to explain the origins of AD, developing an effective strategy in AD clinical therapy is difficult. However, the potential link between AD and circRNA-associated-ceRNA networks provides a new hint in combating this life-threatening disease. Lukiw[13] reported that ciRS-7 acts as a competing endogenous miRNA sponge to inhibit miRNA-7 functions in AD-affected brain. Furthermore, Zhao et al.[14] observed the network of ciRS-7-miRNA-7-UBE2A in sporadic AD (SAD) neocortex and hippocampal CA1. To date, only two cases have been reported in this field. Additional research and attention should be paid to this problem.

In the current study, we elucidated circRNA-associated-ceRNA networks in the brain of senescence-accelerated mouse prone 8 (SAMP8) at the 7-month-old stage using deep RNA sequencing (RNA-seq). SAMP8 has an age-related spontaneous deterioration in learning and memory abilities and is often treated as an important

Received 17 April 2017; accepted 9 June 2017;
http://dx.doi.org/10.1016/j.ymthe.2017.06.009.

Correspondence: Wensheng Zhang, Beijing Normal University, C Building, Beijing Normal University Science Park, No. 12, Xueyuan Southern Street, Haidian District, Beijing 100088, China.
E-mail: zws@bnu.edu.cn

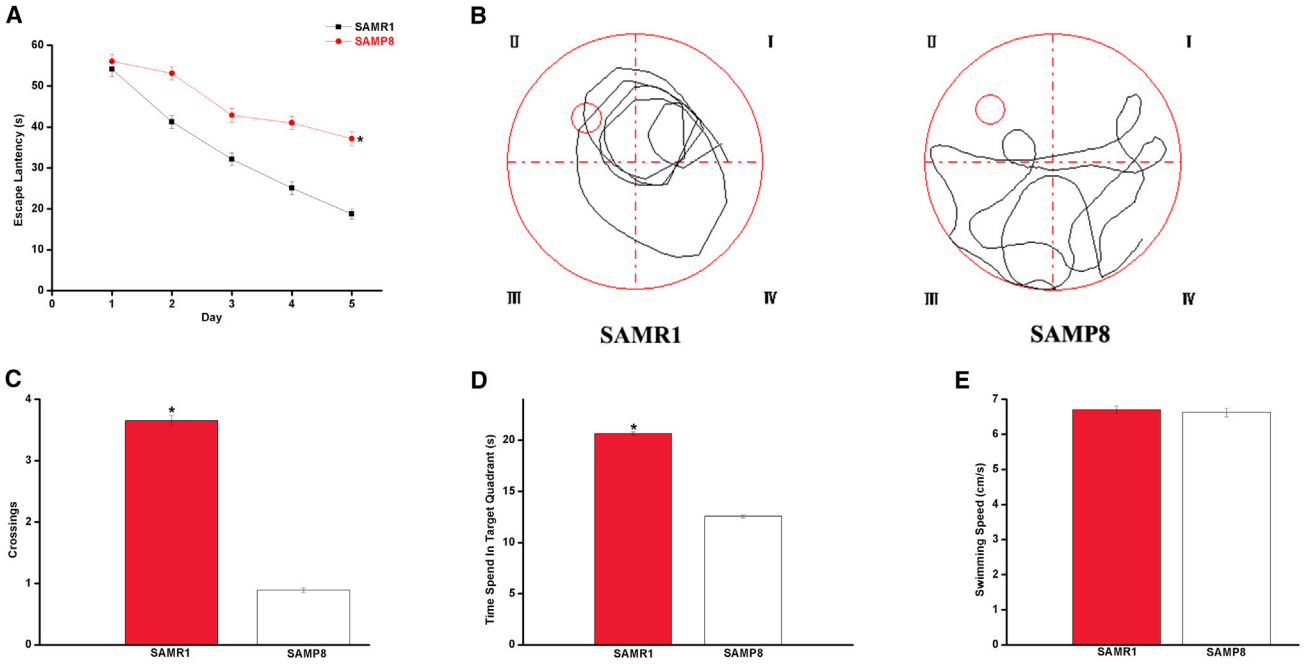

Figure 1. Memory and Learning Ability Evaluation in the SAMP8 Mouse Model

We used the MWM test to evaluate the learning and memory ability in SAMP8 and SAMR1 of 7-month-old mice. (A) Mean escape latency in the hidden platform test. (B) Swimming paths in the probe trial test. (C) Number of crossings in the probe trial test. (D) Time spent in the target quadrant in the probe trial test. (E) Average swimming speeds of mice in the visible-platform test. The data were presented as the mean ± SEM; *$p < 0.05$.

SAD model.[15,16] Senescence-accelerated mouse resistant 1 (SAMR1) is widely used as a control strain.[17] Moreover, RNA-seq is an advanced approach that determines the differential expression profiles underlying phenotypic differences.[18,19] This study is the first to identify circRNA-associated-ceRNA networks in SAD model mice SAMP8, and our data will serve as useful resources for developing therapeutic targets or novel diagnostics in the future.

RESULTS

Memory and Learning Ability Evaluation in the SAMP8 Mouse Model

We used the Morris water maze (MWM) test to evaluate the learning and memory ability in SAMP8 and SAMR1 of 7-month-old mice. As shown in Figure 1A, the mean escape latency of SAMR1 mice significantly decreased compared with that of SAMP8 mice ($p < 0.05$). After the place navigation test, we used the spatial probe test to detect memory retention and spatial exploration ability. As shown in Figure 1B, the SAMP8 mice randomly swam in the tank without knowing the target location, whereas the SAMR1 mice preferentially searched for the target quadrant. Moreover, the number of crossings and the time spent in the target quadrant significantly decreased in the SAMP8 mice compared with those in the SAMR1 mice ($p < 0.05$, Figures 1C and 1D). We did not observe any significant difference in the swimming speed of the two groups ($p > 0.05$, Figure 1E), implying that the cognitive dysfunction of SAMP8 mice was not due to the motor and visual impairments. Compared with the SAMR1 mice of the same age, the 7-month-old SAMP8 mice exhibited severe cognitive impairments, which are the core clinical features observed in AD patients.

Overview of circRNA-Seq

A total of 235,801,234 raw reads (111,956,771 for SAMP8 and 123,844,463 for SAMR1) were generated. We removed the ploy-N-containing, low-quality, and adapter-containing reads from the raw data. A total of 225,282,945 clean reads (118,620,626 for SAMR1 and 106,662,319 for SAMP8) were found in the two groups. The high-quality clean data were mapped to the mouse reference sequence by TopHat v.2.0.9,[20] and the unmapped reads were subsequently selected. Based on the theory of find_circ software,[3] 34,096 circRNAs were detected. These circRNAs were used for the subsequent analysis.

Overview of miRNA-Seq

A total of 72,201,113 raw reads (35,207,345 for SAMP8 and 36,993,768 for SAMR1) were generated. After removal of low-quality and adapter sequences, 71,044,988 clean reads (36,446,427 for SAMR1 and 34,598,561 for SAMP8) were obtained. We filtered the preceding results based on length (18–35 nt). Most selected reads were 22 nt in length for both groups (Figures S1A and S1B). These filtered reads were mapped to the mouse reference sequence by Bowtie,[21] and the mapping rates were approximately 93.67% and 93.51% for the SAMP8 and SAMR1 mice, respectively. These mapped tags were annotated and classified by aligning with non-coding small

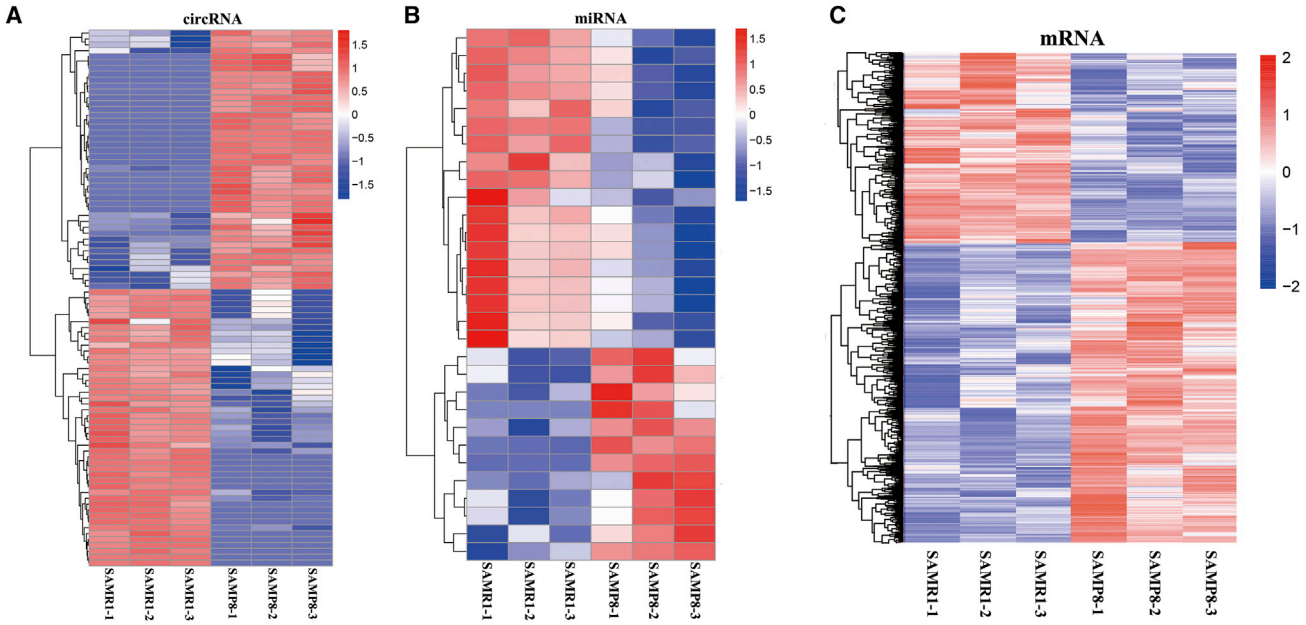

Figure 2. Cluster Analysis Using a Heatmap

(A) Cluster analysis of differentially expressed circRNAs. (B) Cluster analysis of differentially expressed miRNAs. (C) Cluster analysis of differentially expressed mRNAs. Red indicates increased expression, and blue indicates decreased expression.

RNAs (sRNAs) (rRNA, tRNA, small nuclear RNA [snRNA], and small nucleolar RNA [snoRNA]) in GenBank, repeat-associated RNA, exon- and intron-associated RNAs, and miRBase v.20.0. The miREvo[22] and miRDeep2[23] software were integrated to predict the novel miRNA. Finally, 1,298 matured miRNAs (1,226 known and 72 novel) were detected. These miRNAs were used for the subsequent analysis.

Overview of mRNA-Seq

A total of 619,062,690 raw reads (251,783,324 for SAMP8 and 367,279,366 for SAMR1) were generated. After discarding the reads with adapters, poly-N > 10%, and any other possible contaminants, 599,985,802 clean reads (244,770,474 for SAMP8 and 355,215,328 for SAMR1) were obtained. The clean reads were mapped to the mouse reference genome, and the mapping rates were approximately 85.73% and 83.55% for the SAMP8 and SAMR1 mice, respectively. The cufflink results indicated that 74,885 protein-coding transcripts were identified. These mRNAs were used for the subsequent analysis.

Differential Expression Analysis: SAMP8 versus SAMR1

In transcripts per million (TPM), we first identified 235 significantly dysregulated circRNA transcripts between the two groups ($p < 0.01$, Table S2), with 94 upregulated and 141 downregulated transcripts in SAMP8 mice relative to those in SAMR1 mice. Cluster analysis of differentially expressed circRNAs was conducted with a heatmap (Figure 2A). Thirty significantly dysregulated miRNAs were also detected between the two groups based on TPM ($p < 0.01$, Table S3). Twelve dysregulated miRNAs were upregulated in the SAMP8 mice, whereas 18 were upregulated in the SAMR1 mice. Cluster analysis of differentially expressed miRNAs was revealed by a heatmap (Figure 2B). We used fragments per kilobase of exons per million fragments mapped (FPKM) to estimate the expression level of the mRNA transcripts. A total of 1,202 significantly dysregulated mRNA transcripts were identified: 716 were upregulated and 486 were downregulated in SAMP8 mice ($p < 0.01$, Table S4). The cluster analysis of differentially expressed mRNAs is shown in Figure 2C.

qPCR Confirmation

We sought to confirm the differential expression identified in our RNA-seq experiments using qPCR. Nine differentially expressed transcripts were randomly selected: three circRNAs, three miRNAs, and three mRNAs. As shown in Figure 3, all selected transcripts were detected in SAMP8 and SAMR1 brains and exhibited significant differential expressions. In summary, a high level of consistency was observed between the qPCR results and the RNA-seq data.

Construction of a circRNA-Associated-ceRNA Network

According to ceRNA hypothesis, RNA transcripts effectively communicate with one another. The members of ceRNA compete for the same miRNA response elements (MREs) to regulate one another. In this study, we pioneered the identification of a ceRNA network in the SAMP8 brain through our RNA-seq data. We selected 235 circRNAs and 1,202 mRNAs that were differentially expressed and shared a common binding site of MRE (30 significantly dysregulated miRNAs). The ceRNA network covered two cases (Figures 4A and 4B): one was circRNA (up in SAMP8 mice)-miRNA (down in

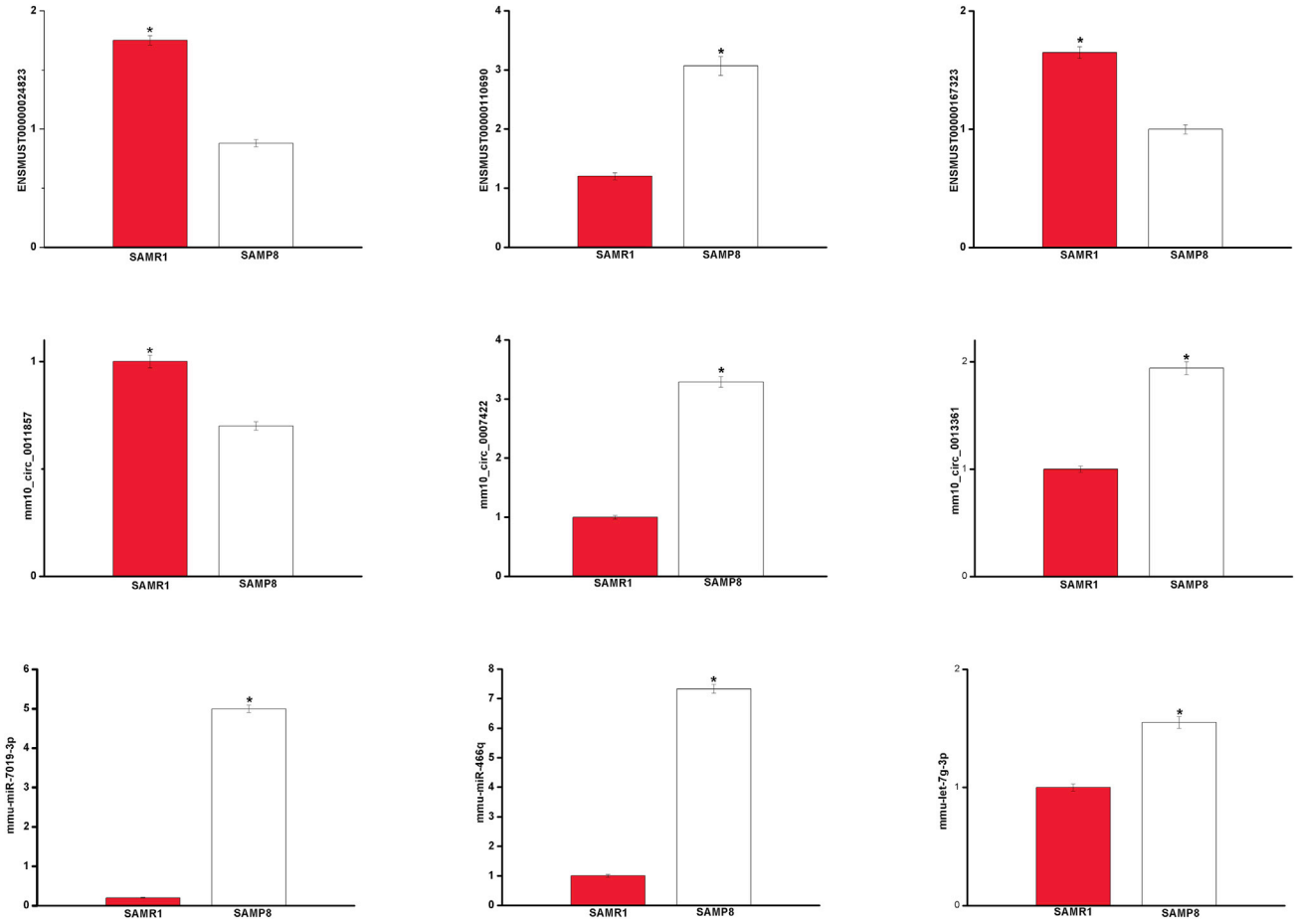

Figure 3. Validation of Transcript Expression by qPCR between SAMP8 and SAMR1 Mice

Mouse β-actin and U6 genes were used as housekeeping internal control. Transcript expression was quantified relative to the expression level of β-actin using the comparative cycle threshold (ΔCT) method. The data were presented as the mean ± SEM (n = 3); *p < 0.05.

SAMP8 mice)-mRNA (up in SAMP8 mice), and the other one was circRNA (down in SAMP8 mice)-miRNA (up in SAMP8 mice)-mRNA (down in SAMP8 mice). Additional details are listed in Tables S5 and S6. These RNA interactions may supply a novel perspective for the pathogenesis of AD.

Functional Annotation: GO

A circRNA-associated-ceRNA network executes functions that are embodied in related mRNA genes. Gene Ontology (GO) analyses were performed on these genes. Through the GO survey, 159 GO terms were significantly enriched (corrected $p < 0.05$, Table S7). The top three terms were intracellular (GO: 0005622), intracellular part (GO: 0044424), and metabolic process (GO: 0008152). Several cognition-associated terms were also observed, such as axon terminus (GO: 0043679), synapse (GO: 0045202), neuron projection terminus (GO: 0044306), axon part (GO: 0033267), and long-term synaptic depression (GO: 0060292). In summary, the circRNA-associated-ceRNA network participates in the pathological progress of AD from different angles.

Association Study

In this study, three limiting factors were established to further understand the most possible relationship between circRNA-associated-ceRNA networks and AD. First, we selectively analyzed pairs in which the circRNAs, miRNAs, and their target genes should be significantly and differentially expressed between the SAMP8 and the SAMR1 mice (corrected $p < 0.05$). Second, the concentrations of the selected circRNAs, miRNAs, and their target genes in the mouse brain should be in a certain order of magnitude. Lastly, the selected pairs should be associated with AD. The fulfilled pairs were detected according to the three preceding requirements. For example, mm10_circ_0027491, mmu_circ_0001293, mm10_circ_0027459, mmu_circ_0000967, and mm10_circ_0027483 were ceRNA of mmu-miR-122-5p targeting Dio2. The expression of Dio2 in AD patients was lower than that in non-AD people.[24] Dio2 activates the thyroid hormone by converting the pro-hormone thyroxine (T4) to bioactive 3,3′,5-triiodothyronine (T3).[25] An increase in thyroxine activates myelination.[26] Myelin sheath loss in AD is a marked morphological component of the disease.[27]

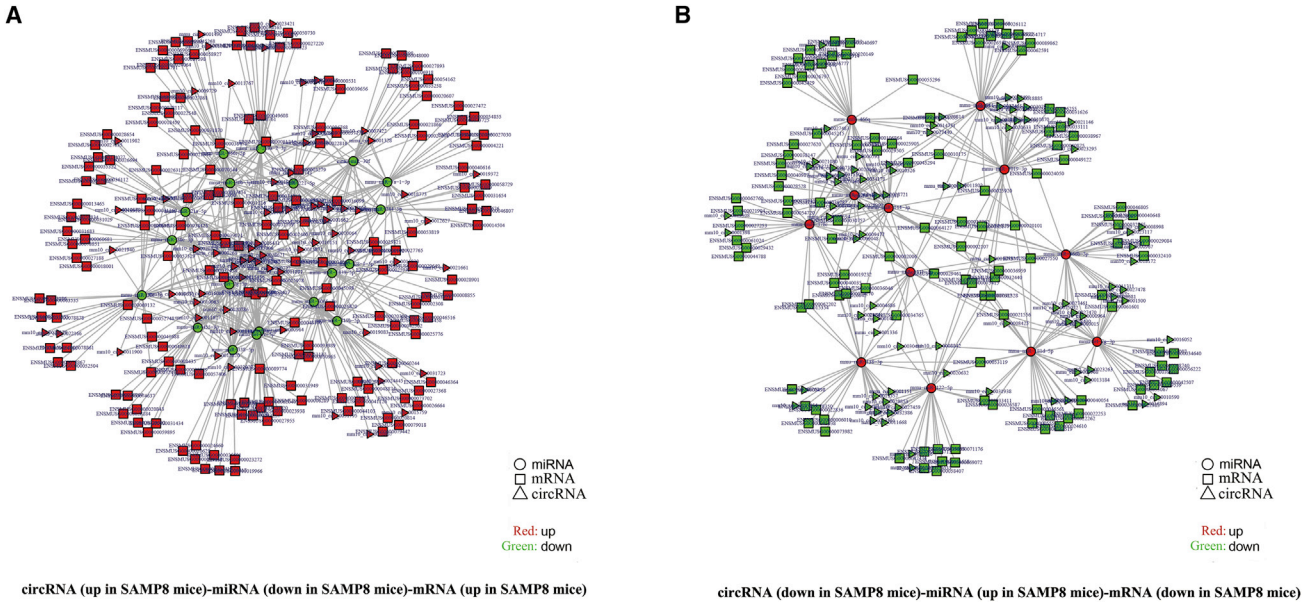

Figure 4. circRNA-Associated-ceRNA Networks in SAMP8 Mice

The ceRNA networks were based on circRNA-miRNA and miRNA-mRNA interactions. (A) circRNA (up in SAMP8 mice)-miRNA (down in SAMP8 mice)-mRNA (up in SAMP8 mice). (B) circRNA (down in SAMP8 mice)-miRNA (up in SAMP8 mice)-mRNA (down in SAMP8 mice).

Additional results are listed in Table 1. Therefore, we predicted that the previously mentioned circRNA-associated-ceRNA networks are possibly involved in the adjustment of AD.

DISCUSSION

AD is a chronic neurodegenerative disease that usually starts slowly and worsens over time.[28] This illness brings huge pain and inconvenience to the patients, including problems with language, behavioral issues, loss of motivation, inability for self-care, and heavy family burdens. However, few therapeutic options are available to prevent or reverse AD because of its complex pathogenesis. The traditional treatment of AD may not be useful in warding off this illness. For example, the protocols targeting the main neuropathological hallmarks in AD (β-amyloid [Aβ] and neurofibrillary tangles) have been unsuccessful.[29] Many studies on AD focused on the epigenetic regulation of its pathogenesis and the potential targets for therapy. The dynamic changes of DNA methylation and long non-coding RNAs (lncRNAs) in brain contribute to AD, as reported by our previous studies.[30,31] However, the occurrence of circRNAs in AD remains largely unknown. The studies of Lukiw[13] and Zhao et al.[14] are the only explorations in this respect. The first evidence about the existence of circRNAs was declared in 1976[32] and was long dismissed as low abundance splicing errors with no function. RNA-seq,[18,19] an up-to-date technology, propels circRNA into the spotlight as a popular topic in the RNA field. Research has shown that the most important function of circRNA is to act as miRNA sponges. circRNAs harbor MREs that can compete with mRNAs for the limited pool of cellular miRNAs and thus affect the level of competing RNAs.[5] circRNAs are more enriched in mammalian brain tissues,[9] implying their important roles in neurodegenerative diseases. In our study, we used RNA-seq to systematically analyze circRNA, miRNA, and mRNA profiles in the 7-month-old SAMP8 mice brain. The 7-month-old SAMP8 mice exhibited the cognitive, behavioral, and neuropathological alterations observed in aged humans and thus are an appropriate animal model to understand the pathogenic mechanisms of AD, especially SAD.[15,16] Our MWM experiment confirmed this result. By contrast, the transgenic mouse models of AD, such as 3xTg-AD (APP/PS1/Tau) and 2xTg-AD (APP/PS1), may simply represent uncommon familial AD (FAD). The circRNA-associated-ceRNA networks were then constructed based on the analysis of the relationship. According to the results, these selected circRNA-associated-ceRNA networks may offer hope of new cues for AD.

Previous research indicated that AD is a multifactorial disease, and many theories, including Aβ deposition, oxidative stress, tau neuropathology, synapse injury, mitochondrial dysfunction, neuron loss, and immune system dysfunction tried to explain the origin of this illness.[33] Many genes are closely related with these theories. Thus, we first explained the significant difference in the gene expression between SAMP8 and SAMR1 brains. A total of 1,202 significantly dysregulated mRNA transcripts were identified. These mRNA transcripts are related to AD pathogenesis. For instance, the Cd274 gene participates in the immunological process.[34] The Cd74 gene suppresses Aβ deposition.[35] In the next two sections, we discussed differential circRNA and miRNA expressions between SAMP8 and SAMR1 mice. According to the statistics, 235 significantly dysregulated circRNA transcripts and 30 significantly

Table 1. circRNA-Associated-ceRNA Networks that Are Most Likely Involved in AD Pathogenesis

circRNA	Log2 Fold Change (SAMP8 versus SAMR1)	Corrected p Value	miRNA	Log2 Fold Change (SAMP8 versus SAMR1)	Corrected p Value	transcript_id	gene_id	gene_name	Log2 Fold Change (SAMP8 versus SAMR1)	Corrected p Value
mm10_circ_0027491	−2.84	3.83E-08								
mmu_circ_0001293	−7.23	8.74E-06								
mm10_circ_0027459	−2.21	0.004122	mmu-miR-122-5p	1.18	0.045558	ENSMUST00000082432	ENSMUSG00000007682	Dio2	−0.37	0.0227923
mmu_circ_0000967	−1.65	0.0064198								
mm10_circ_0027483	−3.36	0.0073264								
mm10_circ_0027470	−6.46	0.0003266								
mm10_circ_0011311	−3.03	0.0068371	mmu-let-7g-3p	0.86	0.0166	ENSMUST00000067925	ENSMUSG00000054717	Hmgb2	−0.64	0.045214
mm10_circ_0018430	−3.65	0.038051								

To make the fold change values easier to work with, a log2 transformation is applied.

dysregulated miRNAs were detected. circRNA and miRNA molecules may be key regulators of diverse AD course. circRNA and protein-coding mRNA function as ceRNAs and super-sponges to regulate the expression of mRNA. Based on this theory, we constructed the most comprehensive miRNA-circRNA and protein-coding mRNA interaction networks of SAMP8 and SAMR1 mice brain. GO analyses revealed that the pathological process of AD may be regulated by these networks from different aspects, including synapse (GO: 0045202), neuron projection terminus (GO: 0044306), axon part (GO: 0033267), and long-term synaptic depression (GO: 0060292).

Strict limitative requirements were applied to select the most possible circRNA-associated-ceRNA networks that are involved in the occurrence and development of AD. Ultimately, two eligible pairs were identified. Earlier in the article, we discussed a network that participates in the control of the Dio2 gene.[24–27] Another one is the Hmgb2 gene. mm10_circ_0027470, mm10_circ_0011311, mm10_circ_0018430, mm10_circ_0009478, mm10_circ_0010326, and mmu_circ_0001442 were ceRNAs of mmu-let-7g-3p targeting Hmgb2. The Hmgb2 gene encoded a member of the non-histone chromosomal high-mobility group protein family.[36] Yamanaka et al.[37] found that Hmgb2 contributes to the expression of the Lrp1 gene. Lrp1 is implicated in the systemic clearance of Aβ, and the level of Lrp1 expression is critical for AD progression.[38] The circRNA-associated-ceRNA networks in AD are highly complex and diverse. Our ongoing efforts will provide more fundamental information for understanding this regulatory mechanism in AD. This endeavor will be an enormous challenge in the future.

In addition, we sought to confirm the differential expressions of the randomly selected transcripts (three circRNAs, three miRNAs, and three mRNAs) identified in RNA-seq experiments using qPCR. The real-time qPCR data agreed with the RNA-seq assay. All of these results confirm that our resultant transcripts were of high quality.

We elucidated the brain circRNA-associated-ceRNA profiles of SAMP8 and SAMR1 mice using deep RNA-seq analysis. Our findings further expanded our knowledge on ceRNA biology and contributed to the understanding of their regulation roles in AD pathogenesis. These novel networks are potential biomarkers or therapeutic targets in AD. Regardless, this strategy should provide a valuable resource for the clinical diagnosis, treatment, and prevention of AD.

MATERIALS AND METHODS

Preparation of Tissues

Three-month-old SAMP8 mice (male, n = 45) and SAMR1 mice (male, n = 45) were purchased from WTLH Biotechnology. The mice were housed one per cage with standard specific conditions (25°C, 50% humidity, 12 hr light/dark cycle, and pathogen free). The mice were provided free diet for 4 months (until they were 7 months old). Three randomly selected animals from each group

were administered general anesthesia. We collected their cerebral cortex for RNA-seq. In addition, we randomly selected 12 animals from each group for the MWM test.

All animal procedures were conducted in accordance with the Guide for the Care and Use of Laboratory Animals[39] and were approved by the Institutional Animal Use and Care Committee of Beijing Normal University.

MWM Test

Spatial learning and memory were evaluated through the MWM test according to standard procedures.[40] One day before the experiment, the mice were familiarized with the MWM environment in the morning and afternoon. In the place navigation test (days 1 to 6), a platform was placed in a set quadrant and submerged 1 cm below the water level. The mice were placed in the maze at four assigned points (southeast, northeast, southwest, and northwest) and allowed to swim for 90 s in every training session. Escape latency was designated as the length of time needed by the mouse to reach the platform. When a mouse failed to reach the platform within 90 s, we guide it toward the platform, and the escape latency was recorded as 90 s. In both cases, the mice were allowed to rest on the platform for 15 s and subsequently placed in the home cage. The mice were subjected to two trials per day for 6 consecutive days. In the spatial probe test (day 7), the platform was withdrawn. The mice were released from the opposite quadrant and allowed to swim freely for 60 s. The swimming trajectory and the number of crossings of the platform within 1 min were recorded. The visible platform test was performed on the day following the spatial probe test (day 8). We raised the platform above the water surface, and each mouse was subjected to four trials. All experiments were conducted at the same time each day. Furthermore, the investigator was unaware of the mouse genotypes until all tests were completed.

RNA Extraction and Qualification

In this study, the total RNA of each sample was isolated using TRIzol reagent (Invitrogen) according to the manufacturer's instructions. Briefly, 1% agarose gels were used to monitor RNA degradation and contamination. RNA purity was checked using the NanoPhotometer spectrophotometer (Implen). RNA concentration was measured using the Qubit RNA Assay Kit in the Qubit 2.0 Fluorometer (Life Technologies). RNA integrity was evaluated by the RNA Nano 6000 Assay Kit of the Bioanalyzer 2100 System (Agilent Technologies).

RNA-Seq

The details of the method for mRNA-seq were previously described.[41] For miRNA-seq and circRNA-seq, the detailed methods are described in Supplemental Materials and Methods.

Expression Analysis

First, we calculated the FPKM of the transcripts using Cuffdiff (v.2.1.1) to evaluate the expression level of protein-coding genes in each sample.[42] The expression levels of miRNAs and circRNAs were estimated by TPM through the following criteria.[43] Transcripts with p value < 0.01 were described as differentially expressed between SAMP8 and SAMR1:

$$\text{Normalized expression} = (\text{mapped reads})/(\text{total reads}) \times 1,000,000.$$

ceRNA Network Analysis

The expression levels of circRNAs, miRNAs, and mRNAs showed significant difference between SAMP8 and SAMR1 and thus were analyzed. The potential MREs were searched on the sequences of circRNAs and mRNAs. We used miRanda (http://www.microrna.org/microrna/) to predict miRNA binding seed sequence sites, and overlapping of the same miRNA binding site on both circRNAs and mRNA represented circRNA-miRNA-mRNA interaction.

GO Enrichment Analyses

The GO database was used to analyze the circRNA-miRNA-enriched genes. GO analysis was performed by the GOseq R package.[44] GO terms with corrected $p < 0.05$ were considered significantly enriched.

Real-Time qPCR Validation

The real-time qPCR reaction was performed using the SYBR Green assay (Cat. No. GMRS-001, GenePharma) in a Light Cycler 480 real-time PCR system (Roche Applied Science) with the following conditions: 95°C for 3 min, followed by 40 cycles of 95°C for 12 s and 62°C for 40 s. Each reaction involved 7.44 μL of H_2O, 0.4 μL of Taq DNA polymerase, 0.08 μL of each primer, 2 μL of cDNA, and 10 μL of 2× RealMasterMix (GenePharma). The specific quantitative primers were designed using oligo7 software and are listed in Table S1. The primers of β-actin (for circRNA and mRNA) and U6 (for miRNA) were designed as an endogenous control. Each experiment was performed in triplicate.

Statistical Analysis

Statistical analyses were performed with SPSS 20.0 software. All data were expressed as the mean ± SEM. $p < 0.05$ was statistically significant. The escape latency in the MWM test was compared through two-way ANOVA. Student's t test was used to compare the qPCR results and the remaining data of the MWM test.

ACCESSION NUMBERS

The accession number for the mRNA-seq, miRNA-seq, and circRNA-seq data reported in this paper are SRA: SRP096779, SRP107885, and SRP107902.

SUPPLEMENTAL INFORMATION

Supplemental Information includes Supplemental Materials and Methods, one figure, and seven tables and can be found with this article online at http://dx.doi.org/10.1016/j.ymthe.2017.06.009.

AUTHOR CONTRIBUTIONS

S.Z. and W.Z. designed the experiments. S.Z. and D.Z. performed the experiments. S.Z. analyzed the data and wrote the paper. S.Z., D.Z., Hong Li, Hejian Li, C.F., and W.Z. contributed reagents, materials, and analysis tools.

CONFLICTS OF INTEREST

We declared that no competing interests exist.

ACKNOWLEDGMENTS

We thank all contributors to this study. This work was supported by the Beijing Joint Project for the Central-Affiliated University (2017-01), the Key New Drug Creation and Development Program of China (2012ZX09103-201), the Fundamental Research Funds for Central Universities (2015KJJCA05), and a grant from the National Natural Science Foundation of China (81274118).

REFERENCES

1. Jeck, W.R., and Sharpless, N.E. (2014). Detecting and characterizing circular RNAs. Nat. Biotechnol. *32*, 453–461.
2. Chen, L.L., and Yang, L. (2015). Regulation of circRNA biogenesis. RNA Biol. *12*, 381–388.
3. Memczak, S., Jens, M., Elefsinioti, A., Torti, F., Krueger, J., Rybak, A., Maier, L., Mackowiak, S.D., Gregersen, L.H., Munschauer, M., et al. (2013). Circular RNAs are a large class of animal RNAs with regulatory potency. Nature *495*, 333–338.
4. Salzman, J., Chen, R.E., Olsen, M.N., Wang, P.L., and Brown, P.O. (2013). Cell-type specific features of circular RNA expression. PLoS Genet. *9*, e1003777.
5. Hansen, T.B., Jensen, T.I., Clausen, B.H., Bramsen, J.B., Finsen, B., Damgaard, C.K., and Kjems, J. (2013). Natural RNA circles function as efficient microRNA sponges. Nature *495*, 384–388.
6. Huang, M., Zhong, Z., Lv, M., Shu, J., Tian, Q., and Chen, J. (2016). Comprehensive analysis of differentially expressed profiles of lncRNAs and circRNAs with associated co-expression and ceRNA networks in bladder carcinoma. Oncotarget *7*, 47186–47200.
7. Fan, X., Weng, X., Zhao, Y., Chen, W., Gan, T., and Xu, D. (2017). Circular RNAs in cardiovascular disease: an overview. BioMed Res. Int. *2017*, 5135781.
8. Peng, L., Chen, G., Zhu, Z., Shen, Z., Du, C., Zang, R., Su, Y., Xie, H., Li, H., Xu, X., et al. (2017). Circular RNA ZNF609 functions as a competitive endogenous RNA to regulate AKT3 expression by sponging miR-150-5p in Hirschsprung's disease. Oncotarget *8*, 808–818.
9. You, X., Vlatkovic, I., Babic, A., Will, T., Epstein, I., Tushev, G., Akbalik, G., Wang, M., Glock, C., Quedenau, C., et al. (2015). Neural circular RNAs are derived from synaptic genes and regulated by development and plasticity. Nat. Neurosci. *18*, 603–610.
10. Braak, H., and Del Trecidi, K. (2015). Neuroanatomy and pathology of sporadic Alzheimer's disease. Adv. Anat. Embryol. Cell Biol. *215*, 1–162.
11. Roy, D.S., Arons, A., Mitchell, T.I., Pignatelli, M., Ryan, T.J., and Tonegawa, S. (2016). Memory retrieval by activating engram cells in mouse models of early Alzheimer's disease. Nature *531*, 508–512.
12. Burns, A., and Iliffe, S. (2009). Alzheimer's disease. BMJ *338*, b158.
13. Lukiw, W.J. (2013). Circular RNA (circRNA) in Alzheimer's disease (AD). Front. Genet. *4*, 307.
14. Zhao, Y., Alexandrov, P.N., Jaber, V., and Lukiw, W.J. (2016). Deficiency in the ubiquitin conjugating enzyme UBE2A in Alzheimer's disease (AD) is linked to deficits in a natural circular miRNA-7 sponge (circRNA; ciRS-7). Genes (Basel) *7*, 116.
15. Kang, L., Li, S., Xing, Z., Li, J., Su, Y., Fan, P., Wang, L., and Cui, H. (2014). Dihydrotestosterone treatment delays the conversion from mild cognitive impairment to Alzheimer's disease in SAMP8 mice. Horm. Behav. *65*, 505–515.
16. Takeda, T. (2009). Senescence-accelerated mouse (SAM) with special references to neurodegeneration models, SAMP8 and SAMP10 mice. Neurochem. Res. *34*, 639–659.
17. Castillo, C.A., Albasanz, J.L., León, D., Jordán, J., Pallàs, M., Camins, A., and Martín, M. (2009). Age-related expression of adenosine receptors in brain from the senescence-accelerated mouse. Exp. Gerontol. *44*, 453–461.
18. Wang, Z., Gerstein, M., and Snyder, M. (2009). RNA-seq: a revolutionary tool for transcriptomics. Nat. Rev. Genet. *10*, 57–63.
19. Marguerat, S., and Bähler, J. (2010). RNA-seq: from technology to biology. Cell. Mol. Life Sci. *67*, 569–579.
20. Kim, D., Pertea, G., Trapnell, C., Pimentel, H., Kelley, R., and Salzberg, S.L. (2013). TopHat2: accurate alignment of transcriptomes in the presence of insertions, deletions and gene fusions. Genome Biol. *14*, R36.
21. Langmead, B., Trapnell, C., Pop, M., and Salzberg, S.L. (2009). Ultrafast and memory-efficient alignment of short DNA sequences to the human genome. Genome Biol. *10*, R25.
22. Wen, M., Shen, Y., Shi, S., and Tang, T. (2012). miREvo: an integrative microRNA evolutionary analysis platform for next-generation sequencing experiments. BMC Bioinformatics *13*, 140.
23. Friedländer, M.R., Mackowiak, S.D., Li, N., Chen, W., and Rajewsky, N. (2012). miRDeep2 accurately identifies known and hundreds of novel microRNA genes in seven animal clades. Nucleic Acids Res. *40*, 37–52.
24. Humphries, C.E., Kohli, M.A., Nathanson, L., Whitehead, P., Beecham, G., Martin, E., Mash, D.C., Pericak-Vance, M.A., and Gilbert, J. (2015). Integrated whole transcriptome and DNA methylation analysis identifies gene networks specific to late-onset Alzheimer's disease. J. Alzheimers Dis. *44*, 977–987.
25. Buettner, C., Harney, J.W., and Larsen, P.R. (2000). The role of selenocysteine 133 in catalysis by the human type 2 iodothyronine deiodinase. Endocrinology *141*, 4606–4612.
26. Calza, L., Fernandez, M., Giuliani, A., Aloe, L., and Giardino, L. (2002). Thyroid hormone activates oligodendrocyte precursors and increases a myelin-forming protein and NGF content in the spinal cord during experimental allergic encephalomyelitis. Proc. Natl. Acad. Sci. USA *99*, 3258–3263.
27. Zhan, X., Jickling, G.C., Ander, B.P., Liu, D., Stamova, B., Cox, C., Jin, L.W., DeCarli, C., and Sharp, F.R. (2014). Myelin injury and degraded myelin vesicles in Alzheimer's disease. Curr. Alzheimer Res. *11*, 232–238.
28. Scheltens, P., Blennow, K., Breteler, M.M., de Strooper, B., Frisoni, G.B., Salloway, S., and Van der Flier, W.M. (2016). Alzheimer's disease. Lancet *388*, 505–517.
29. Selkoe, D.J. (2011). Resolving controversies on the path to Alzheimer's therapeutics. Nat. Med. *17*, 1060–1065.
30. Zhang, S., Qin, C., Cao, G., Guo, L., Feng, C., and Zhang, W. (2017). Genome-wide analysis of DNA methylation profiles in a senescence-accelerated mouse prone 8 brain using whole-genome bisulfite sequencing. Bioinformatics *33*, 1591–1595.
31. Zhang, S., Qin, C., Cao, G., Xin, W., Feng, C., and Zhang, W. (2016). Systematic analysis of long noncoding RNAs in the senescence-accelerated mouse prone 8 brain using RNA sequencing. Mol. Ther. Nucleic Acids *5*, e343.
32. Sanger, H.L., Klotz, G., Riesner, D., Gross, H.J., and Kleinschmidt, A.K. (1976). Viroids are single-stranded covalently closed circular RNA molecules existing as highly base-paired rod-like structures. Proc. Natl. Acad. Sci. USA *73*, 3852–3856.
33. Armstrong, R.A. (2013). What causes Alzheimer's disease? Folia Neuropathol. *51*, 169–188.
34. Saresella, M., Calabrese, E., Marventano, I., Piancone, F., Gatti, A., Farina, E., Alberoni, M., and Clerici, M. (2012). A potential role for the PD1/PD-L1 pathway in the neuroinflammation of Alzheimer's disease. Neurobiol. Aging *33*, 624.e11–624.e22.
35. Matsuda, S., Matsuda, Y., and D'Adamio, L. (2009). CD74 interacts with APP and suppresses the production of Abeta. Mol. Neurodegener. *4*, 41.
36. Murugesapillai, D., McCauley, M.J., Maher, L.J., 3rd, and Williams, M.C. (2016). Single-molecule studies of high-mobility group B architectural DNA bending proteins. Biophys. Rev. *9*, 17–40.

37. Yamanaka, Y., Faghihi, M.A., Magistri, M., Alvarez-Garcia, O., Lotz, M., and Wahlestedt, C. (2015). Antisense RNA controls LRP1 Sense transcript expression through interaction with a chromatin-associated protein, HMGB2. Cell Rep. *11*, 967–976.

38. Martiskainen, H., Haapasalo, A., Kurkinen, K.M., Pihlajamäki, J., Soininen, H., and Hiltunen, M. (2013). Targeting ApoE4/ApoE receptor LRP1 in Alzheimer's disease. Expert Opin. Ther. Targets *17*, 781–794.

39. Clark, J.D., Gebhart, G.F., Gonder, J.C., Keeling, M.E., and Kohn, D.F. (1997). Special report: the 1996 guide for the care and use of laboratory animals. ILAR J. *38*, 41–48.

40. Vorhees, C.V., and Williams, M.T. (2006). Morris water maze: procedures for assessing spatial and related forms of learning and memory. Nat. Protoc. *1*, 848–858.

41. Zhang, S., Zhu, D., Li, H., Zhang, H., Feng, C., and Zhang, W. (2017). Analyses of mRNA profiling through RNA sequencing on a SAMP8 mouse model in response to ginsenoside Rg1 and Rb1 treatment. Front. Pharmacol. *8*, 88.

42. Trapnell, C., Williams, B.A., Pertea, G., Mortazavi, A., Kwan, G., van Baren, M.J., Salzberg, S.L., Wold, B.J., and Pachter, L. (2010). Transcript assembly and quantification by RNA-seq reveals unannotated transcripts and isoform switching during cell differentiation. Nat. Biotechnol. *28*, 511–515.

43. Zhou, L., Chen, J., Li, Z., Li, X., Hu, X., Huang, Y., Zhao, X., Liang, C., Wang, Y., Sun, L., et al. (2010). Integrated profiling of microRNAs and mRNAs: microRNAs located on Xq27.3 associate with clear cell renal cell carcinoma. PLoS ONE *5*, e15224.

44. Young, M.D., Wakefield, M.J., Smyth, G.K., and Oshlack, A. (2010). Gene ontology analysis for RNA-seq: accounting for selection bias. Genome Biol. *11*, R14.

YMTHE, Volume *25*

Supplemental Information

Characterization of circRNA-Associated-ceRNA Networks in a Senescence-Accelerated Mouse Prone 8 Brain

Shuai Zhang, Dina Zhu, Hong Li, Hejian Li, Chengqiang Feng, and Wensheng Zhang

Figure S1

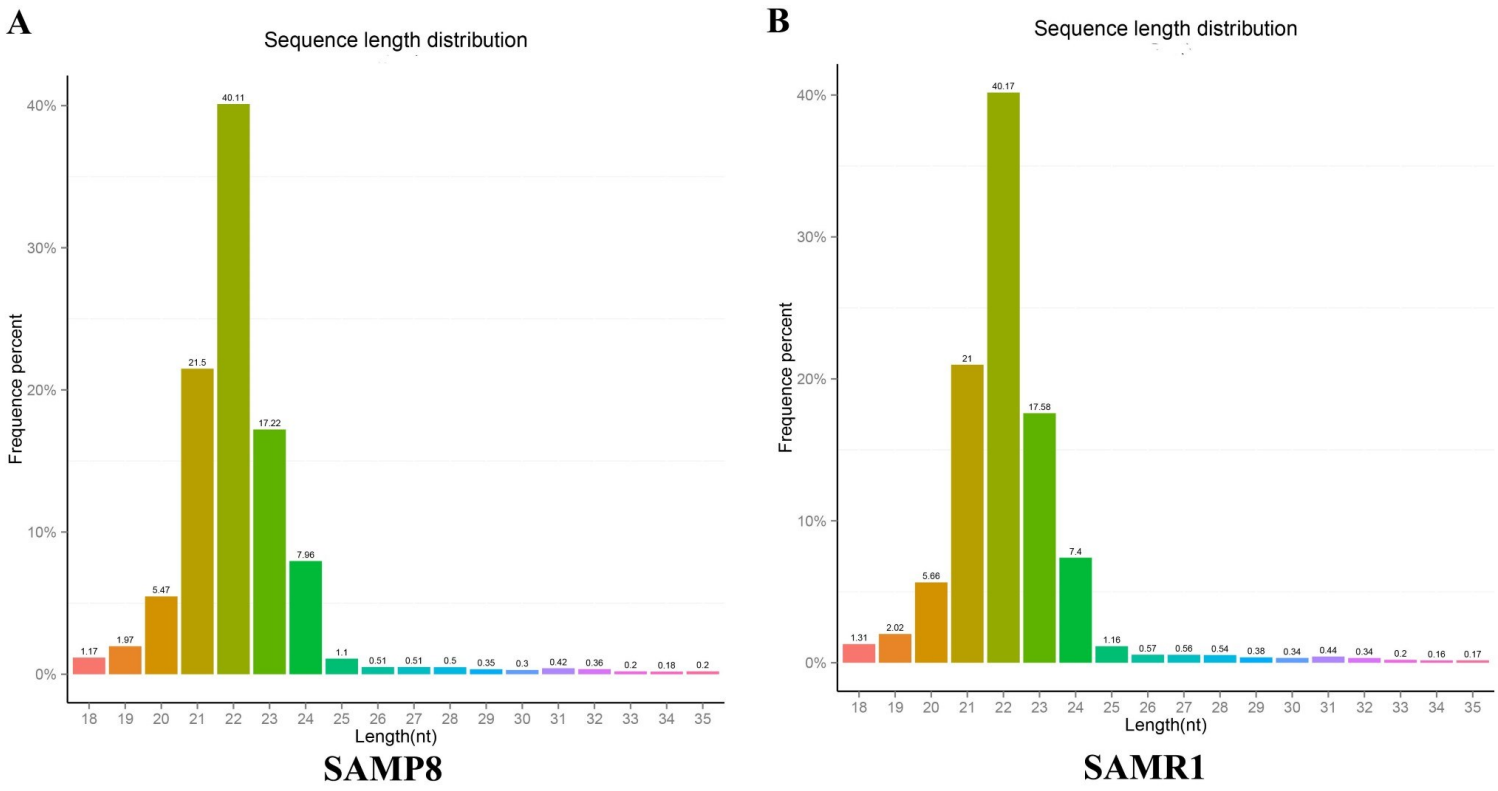

Figure S1. Sequence length distribution of small RNA in SAMP8 and SAMR1 mice. (A) Sequence length distribution in SAMP8 mice. (B) Sequence length distribution in SAMR1 mice.

Table S1. Primers used in qPCR analysis

Acession No.	Primer sequence (5`-3`)	primer direction	product size
ENSMUST00000024823	CGGCTACTGGATTGAGA	forward primer	99
	CTTTGTTCCCGCTGTC	reverse primer	
ENSMUST00000110690	AAACTCCTGTCCTCTGGGCTTCG	forward primer	142
	ATCTTTTACAGCTTCCACGGGAT	reverse primer	
ENSMUST00000167323	CATCGTCTTCTTCGGCTCAC	forward primer	152
	GCTGCTCACTAAGTTCATCCA	reverse primer	
mm10_circ_0011857	ATGGTCTGGTCGGCAAGC	forward primer	106
	GAGCGATGGGTCGTAGGTAA	reverse primer	
mm10_circ_0007422	TGATGATATCCGCCCAGACA	forward primer	106
	CAGGACTAAAACTTCTCGCACTG	reverse primer	
mm10_circ_0013361	AGACAGTGATCCTCCCATTCA	forward primer	136
	TTCTTCAGACATCATCAGTGGC	reverse primer	
mmu-miR-7019-3p	ACATATATCACCTTGGCCGCC	forward primer	74
	TATGGTTGTTCACGACTCCTTCAC	reverse primer	
mmu-miR-466q	GGCAAGTGCACACACACAC	forward primer	71
	TATGGTTTTGACGACTGTGTGAT	reverse primer	
mmu-let-7g-3p	GCACATACATGGTGCACACACA	forward primer	70
	TATGGTTGTTCACGACTCCTTCAC	reverse primer	
U6	CAGCACATATACTAAAATTGGAACG	forward primer	76
	ACGAATTTGCGTGTCATCC	reverse primer	
β-Actin	GCCCATCTACGAGGGCTAT	forward primer	147
	ATGTCACGCACGATTTCC	reverse primer	

Table S3. Significantly and differentially expressed miRNA transcripts between SAMP8 and SAMR1 mice

sRNA	SAMR1_readcount	SAMP8_readcount	$log2^{FoldChange}$	pval
mmu-miR-3086-5p	2.207373438	72.62548772	-3.3761	3.50E-24
mmu-miR-466q	0	23.66608457	-2.6907	5.82E-13
mmu-let-7a-5p	68025.34354	54718.33238	0.31185	6.32E-07
mmu-miR-181d-5p	4965.527081	6006.41333	-0.2723	4.90E-05
mmu-let-7g-5p	448676.6117	368188.6576	0.28232	0.00020599
mmu-miR-344-3p	5177.433908	7226.426387	-0.46674	0.00024286
mmu-miR-221-5p	4562.344165	3809.130442	0.25844	0.00045981
mmu-miR-30e-3p	9940.051867	8161.14345	0.28151	0.00050191
mmu-miR-219b-5p	2155.285501	1208.686225	0.75696	0.0005365
mmu-miR-144-3p	15.74204162	65.87510204	-1.2477	0.00069635
mmu-miR-122-5p	26.55221656	89.89337916	-1.1781	0.00086852
mmu-miR-551b-3p	94.71884185	205.0504622	-0.91206	0.0015702
mmu-miR-138-5p	4130.69484	5307.460187	-0.35343	0.0016526
mmu-miR-744-5p	4227.856839	3460.486003	0.28446	0.0020397
mmu-miR-30b-3p	285.6550283	213.8102253	0.40347	0.0023108
mmu-miR-455-3p	170.2339162	118.0757926	0.49072	0.0024029
mmu-miR-3065-3p	1958.957482	1300.204444	0.5529	0.0028
mmu-miR-338-5p	1997.940091	1329.581848	0.54931	0.0029962
mmu-miR-219a-2-3p	12372.53421	8339.371718	0.53416	0.0032678
mmu-miR-466i-5p	29.37106327	9.308007664	1.0404	0.00423
mmu-miR-7a-1-3p	522.9449924	416.9477258	0.31917	0.0045518
mmu-miR-30c-5p	81923.16111	65829.9945	0.30861	0.0052923
mmu-let-7c-5p	123416.9698	101959.5811	0.2709	0.0054639
mmu-miR-21a-5p	48315.68007	36703.76465	0.38273	0.0058751
mmu-miR-7019-3p	0	3.466885077	-0.92191	0.0061499
mmu-let-7g-3p	14.41850254	31.68328894	-0.86017	0.0071926
mmu-miR-466b-5p	2.820977233	9.738081367	-0.99696	0.0075774
mmu-miR-128-1-5p	568.311237	399.8551909	0.47398	0.0084636
mmu-miR-378c	1429.041877	1786.423398	-0.31289	0.0089111
mmu-miR-1839-5p	5148.845716	4363.856225	0.23522	0.0095727

Supplemental Method 1. The detailed methods of miRNA-seq

Library preparation and sequencing

A total of six cDNA libraries were constructed, i.e., three for SAMP8 mice and another three for SAMR1 mice. We utilized 3 μg RNA per sample as input material for RNA sample preparation. Sequencing libraries were generated using NEBNext® Multiplex Small RNA Library Prep Set for Illumina® (NEB, USA.) following manufacturer's recommendations and index codes were added to attribute sequences to each sample. Briefly, NEB 3' SR Adaptor was directly, and specifically ligated to 3' end of miRNA, siRNA and piRNA. After the 3' ligation reaction, the SR RT Primer hybridized to the excess of 3' SR Adaptor (that remained free after the 3' ligation reaction) and transformed the single-stranded DNA adaptor into a double-stranded DNA molecule. This step is important to prevent adaptor-dimer formation, besides, dsDNAs are not substrates for ligation mediated by T4 RNA Ligase 1 and therefore do not ligate to the 5´ SR Adaptor in the subsequent ligation step. 5´ends adapter was ligated to 5´ends of miRNAs, siRNA and piRNA. Then first strand cDNA was synthesized using M-MuLV Reverse Transcriptase (RNase H–). PCR amplification was performed using LongAmp Taq 2X Master Mix, SR Primer for illumina and index (X) primer. PCR products were purified on a 8% polyacrylamide gel (100V, 80 min). DNA fragments corresponding to 140~160 bp (the length of small noncoding RNA plus the 3' and 5' adaptors) were recovered and dissolved in 8 μL elution buffer. At last, library quality was assessed on the Agilent Bioanalyzer 2100 system using DNA High Sensitivity Chips.

The clustering of the index-coded samples was performed on a cBot Cluster Generation System using TruSeq SR Cluster Kit v3-cBot-HS (Illumia) according to the manufacturer's instructions. After cluster generation, the library preparations were sequenced at the Novogene Bioinformatics Institute (Beijing, China) on an Illumina Hiseq 2500/2000 platform and 50bp single-end reads were generated.

Data analysis

This section contained Quality control (QC), Reads mapping to the reference sequence, Known miRNA alignment, Remove tags from these sources (protein-coding genes, repeat sequences, rRNA, tRNA, snRNA, and snoRNA), Novel miRNA prediction, Small RNA annotation summary, miRNA editing analysis, miRNA family analysis, and Target gene prediction.

Supplemental Method 2. The detailed methods of circRNA-seq

Library preparation and sequencing

A total of six cDNA libraries were constructed, i.e., three for SAMP8 mice and another three for SAMR1 mice. We utilized 5 μg RNA per sample as input material for RNA sample preparation. Firstly, ribosomal RNAs were depleted by using Epicentre Ribo-zero™ rRNA Removal Kit (Epicentre, USA) to get rRNA-depleted RNAs. rRNA-depleted RNAs were further treated with RNase R (Epicentre, USA) and then were subjected to Trizol extraction. Subsequently, sequencing libraries were generated using the rRNA-depleted and RNase R digested RNAs by NEBNext® Ultra™ Directional RNA Library Prep Kit for Illumina® (NEB, USA) following manufacturer's recommendations. Briefly, fragmentation was carried out using divalent cations under elevated temperature in NEBNext First Strand Synthesis Reaction Buffer. First strand cDNA was synthesized using random hexamer primer and M-MuLV Reverse Transcriptase (RNaseH-). Second strand cDNA synthesis was subsequently performed using DNA Polymerase I and RNase H. In the reaction buffer, dNTPs with dTTP were replaced by dUTP. Remaining overhangs were converted into blunt ends via exonuclease/polymerase activities. After adenylation of 3' ends of DNA fragments, NEBNext Adaptor with hairpin loop structure were ligated to prepare for hybridization. In order to select cDNA fragments of preferentially 150-200 bp in length, the library fragments were purifed with AMPure XP system (Beckman Coulter, Beverly, USA). Then 3 μl USER Enzyme (NEB, USA) was used with size-selected, adaptor-ligated cDNA at 37°C for 15 min followed by 5 min at 95°C before PCR. PCR was performed with Phusion High-Fidelity DNA polymerase, Universal PCR primer and Index (X) Primer. Finally, the library was purifed (AMPure XP system) and then qualifed by the Agilent Bioanalyzer 2100 system.

The clustering of the index-coded samples was performed on a cBot Cluster Generation System using HiSeq PE Cluster Kit v4 cBot (Illumina) according to the manufacturer's instructions. After cluster generation, the library preparations were sequenced at the Novogene Bioinformatics Institute (Beijing, China) on an Illumina Hiseq 2500 platform and 125bp paired-end reads were generated.

Data analysis

This section contained Quality control (QC), Mapping to reference genome, circRNA identifcation and miRNA binding site prediction.